J Pathol Inform

Editor-in-Chief:
Anil V. Parwani , Columbus, OH, USA
Liron Pantanowitz, Pittsburgh, PA, USA

OPEN ACCESS
HTML format

For entire Editorial Board visit : www.jpathinformatics.org/editorialboard.asp

Original Article

Validation of break-apart and fusion *MYC* probes using a digital fluorescence *in situ* hybridization capture and imaging system

Michael Liew[1], Leslie Rowe[1], Parker W. Clement[1,2], Rodney R. Miles[1,2], Mohamed E. Salama[1,2]

[1]Institute for Clinical and Experimental Pathology, ARUP Laboratories, Salt Lake City, UT 84108, [2]Department of Pathology, University of Utah School of Medicine, Salt Lake City, UT 84132, USA

E-mail: *Dr. Michael Liew - liewm@aruplab.com
*Corresponding author

Received: 13 November 2015 Accepted: 15 March 2016 Published: 04 May 2016

Abstract

Introduction: Detection of *MYC* translocations using fluorescence *in situ* hybridization (FISH) is important in the evaluation of lymphomas, in particular, Burkitt lymphoma and diffuse large B-cell lymphoma. Our aim was to validate a digital FISH capture and imaging system for the detection of *MYC* 8q24 translocations using LSI-MYC (a break-apart probe) and *MYC* 8;14 translocation using IGH-MYC (a fusion probe). **Materials and Methods:** LSI-MYC probe was evaluated using tissue sections from 35 patients. IGH-MYC probe was evaluated using tissue sections from forty patients. Sections were processed for FISH and analyzed using traditional methods. FISH slides were then analyzed using the GenASIs capture and analysis system. **Results:** Results for LSI-MYC had a high degree of correlation between traditional method of FISH analysis and digital FISH analysis. Results for IGH-MYC had a 100% concordance between traditional method of FISH analysis and digital FISH analysis. **Conclusion:** Annotated whole slide images of H and E and FISH sections can be digitally aligned, so that areas of tumor within a section can be matched and evaluated with a greater degree of accuracy. Images can be archived permanently, providing a means for examining the results retrospectively. Digital FISH imaging of the *MYC* translocations provides a better diagnostic tool compared to traditional methods for evaluating lymphomas.

Key words: Break apart probe, fusion probe, GenASIs analysis system

Access this article online

Website: www.jpathinformatics.org

DOI: 10.4103/2153-3539.181764

Quick Response Code:

INTRODUCTION

The *MYC* gene is a promoter of cellular proliferation located at chromosome 8q24. Its oncogenic relevance is appreciated in high-grade B-cell lymphomas (BCLs) where rearrangements occur between *MYC* and immunoglobulin (IG) heavy chain (chromosome 14), kappa light chain (2p11), or lambda light chain (22q11) genes in Burkitt lymphoma.[1,2] *MYC* translocations can also involve non-IG partners in other high-grade BCLs[1-3] including double and triple hit diffuse large BCLs (DLBCLs), and a subset of large BCLs with features intermediate between DLBCL and Burkitt lymphoma.[4] However, it has been reported that approximately half of the cases of double hit DLBCL harbor IG-MYC translocations, with the remainder being non-IG partner genes.[5,6] Double and triple hit large BCLs tend to manifest aggressively with poor response to

This article may be cited as:
Liew M, Rowe L, Clement PW, Miles RR, Salama ME. Validation of break-apart and fusion MYC probes using a digital fluorescence in situ hybridization capture and imaging system. J Pathol Inform 2016;7:20.

Available FREE in open access from: http://www.jpathinformatics.org/text.asp?2016/7/1/20/181764

chemotherapy and appear to have an association with the IG-MYC translocation.[5,6]

MYC translocations can be detected in formalin-fixed paraffin-embedded (FFPE) tissue specimens using either break-apart or fusion fluorescence *in situ* hybridization (FISH) probes. Dual fusion probes are known to be more sensitive than break-apart probes with the chance of obtaining a false-positive result in normal tissue being very close to zero.[7] A significant advantage of the break-apart signal is its ease of recognition in abnormal cells and the detection of *MYC* translocations with various partners including non-IgH. In concordance with the beneficial aspects of both, a retrospective study of 91 aggressive BCLs recommended the use of both IGH-MYC dual fusion and *MYC* break-apart probes[8] for optimal detection of *MYC* translocations.

Detection of chromosomal rearrangements by FISH is well-accepted as a robust and reliable technique for the diagnosis of lymphoma associated translocations.[9] In standard FISH methods, sections are visualized under the microscope and scored by evaluating observed signal patterns. As inferred by its manual mode of operation, this method of scoring cells is both labor intensive and time-consuming, often requiring two individuals, one who visualizes and interprets signal patterns at the microscope and another who tabulates called signals, to expedite the process. Because fluorescent signals on FFPE tissue tend to fade and photobleach with time, the current accepted standard of practice is to capture representative images of selected representative fields using a standard fluorescence microscope with attached camera. This approach, however, does not provide a permanent record of the actual cells being counted or their designated classification.

Another significant disadvantage of traditional microscope-based FISH analysis involves laboratory workflow. In our practice, the standard operating procedure involves specimen receipt with appropriate processing, including preparation of H and E slides and slides for probe application. H and E stained slides are then transported from the histology laboratory to the offices of pathologists where the tissue is morphologically assessed, and tumor is manually annotated by felt-tipped marking pen. The annotated slides are then physically transported back to the FISH laboratory where areas of marked tumor are matched by manually overlaying and etching FISH slides. Technologists tabulate cell signals at the microscope in etched areas and, finally, pathologists physically report to the FISH lab for official sign out of cases.

Automated digital FISH has recently been implemented in a number of diagnostic laboratories.[10-12] With advancing technology, multiple options for digital recording and analysis of FISH images are becoming available. In this study, we report our validation approach for the GenASIs capture and analysis system (Applied Spectral Imaging, Carlsbad, CA, USA) for FISH analysis of *MYC* break-apart (LSI-MYC) and fusion (IGH-MYC) probes. We also report our experience with regards to the advantages and limitations of the digital capture and analysis approach and workflow.

MATERIALS AND METHODS

Formalin-fixed Paraffin-embedded Samples

FFPE samples from 35 patients were analyzed using the LSI-MYC probe in this study. Forty FFPE samples from forty patients were analyzed using the IGH-MYC probe in this study. Samples were selected based on being positive or negative for *MYC* rearrangements by prior manually scored FISH. Samples from 14 of the LSI-MYC samples (56 total punches, 2–9 replicates/sample) were from a tissue microarray that was comprised Burkitt lymphoma samples. The remaining 21 samples were from reference laboratory samples submitted to ARUP for routine hematopathology FISH analysis, and the final diagnosis could not be confirmed. The forty IGH-MYC samples were also samples submitted to ARUP for routine hematopathology FISH analysis. This study was approved by the University of Utah Institutional Review Board #32162.

Upon receipt of a case, sections were prepared for H and E staining and FISH processing. The H and E slide was scanned using an Aperio® AT2 slide scanner (Leica Biosystems, Buffalo Grove, IL, USA). The scanned H and E image was used for morphologic identification and digital annotation of viable tumor, which was then subjected to FISH analysis. In addition, the H and E image was used for digital alignment to a 4′,6-diamidino-2- phenylindole (DAPI) prescan image of the FISH slide for accurate transfer of the annotations. The H and E image was reviewed and annotated using eSlide Manager (Leica Biosystems). Case information was entered into the GenASIs system for slide identification, barcode printing, H and E image tissue matching, and report generation. The H and E and DAPI prescan images were aligned using digital tissue matching techniques to transfer H and E digital annotations to the DAPI prescan image. Using the annotated DAPI prescan image as a guide, ×60 magnified images of the FISH slide were captured and analyzed. Finally, images were reviewed by a laboratory technologist and a pathologist.

Fluorescence *In situ* Hybridization

Five-micron unstained FFPE sections were used for FISH analysis. The 8q24 *MYC* rearrangement is detected using the Vysis LSI-MYC dual color break-apart rearrangement probe kit (Abbott Laboratories, Des Plaines, IL USA). This kit contains a mixture of LSI-MYC SpectrumOrange probe and LSI-MYC SpectrumGreen probe. The t(8;14)(q24;q32)

translocation is detected by the Vysis LSI IGH/MYC/VYSIS chromosome enumeration probe (CEP) 8 tricolor dual fusion probe kit (Abbott Laboratories). This kit contains a mixture of LSI-MYC SpectrumOrange probe, LSI IGH SpectrumGreen probe, and CEP 8 SpectrumAqua probe. On the 1st day, slides were pretreated and hybridized using the VP2000 (SciGene, Sunnyvale, CA, USA) according to manufacturer instructions. The following day, slides were washed using the Little Dipper (Abbott Laboratories). Washed slides were counterstained using Vectashield Mounting Medium with DAPI (Vector Laboratories, Burlingame, CA USA) and coverslipped. Slides were stored at − 20°C if not scored immediately.

Tissue Matching

Before capturing FISH images, adjacent H and E sections were analyzed for regions containing tumor. These areas were circled, and the same regions on the FISH slide were examined for rearranged nuclei. Traditionally, the regions have been circled using a diamond tipped pen, which could lead to variability in the translation of the region to the FISH slide. The GenASIs capture and analysis system has the capability of accurately matching digitally annotated H and E sections with tissue upon scanned FISH slides. Our protocol involved scanning the H and E slide on the Aperio AT scan scope (Leica Biosystems, Buffalo Grove, IL, USA) at ×20 magnification and importing the thumbnail image into the GenASIs system. For matching of the FISH image, the FISH slide was scanned at ×4 magnification using DAPI filter. The two images were then aligned using the GenASIs software [Figure 1].

Image Capture

Following tissue matching, the FISH slide was ready for capturing images that could be used for analysis. These images were captured at ×60 magnification. The instrument settings as shown in Table 1 were used with the GenASIs capture and analysis system for each assay. A sufficient number of fields of view were captured so that at least 100 nuclei were visualized and contained interpretable signal. A minimum of four fields of view was captured per sample.

Fluorescence *In situ* Hybridization Segmentation and Classification

The software analysis is divided into two parts, segmentation, and classification. Segmentation is

Table 1: GenASIs capture and analysis system settings

Instrument setting	LSI-MYC	IGH-MYC
Filter exposure time (ms)		
DAPI	15	15
Green	400	200
Red	400	450
Aqua	N/A	75
Signal sensitivity levels (ms)		
Green	800	800
Red	800	800
Aqua	N/A	1200
Major background fluorescence		
Green	0.2	0.2
Red	0.2	0.15
Aqua	N/A	0.25
Spot gap (%)		
Min spot gap	6.0	6.0
Max spot gap	6.0	6.0

DAPI: diamidino-2- phenylindole, N/A: Not applicable

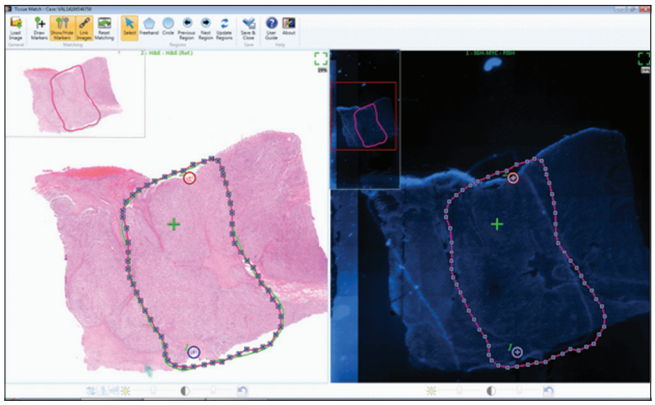

Figure 1: Screen shot of tissue matching software showing the H and E image (left) and 4′,6-diamidino-2- phenylindole prescan image (right) aligned.The annotation has been traced on the H and E image and has been transferred to the 4′,6-diamidino-2- phenylindole prescan image (pink line)

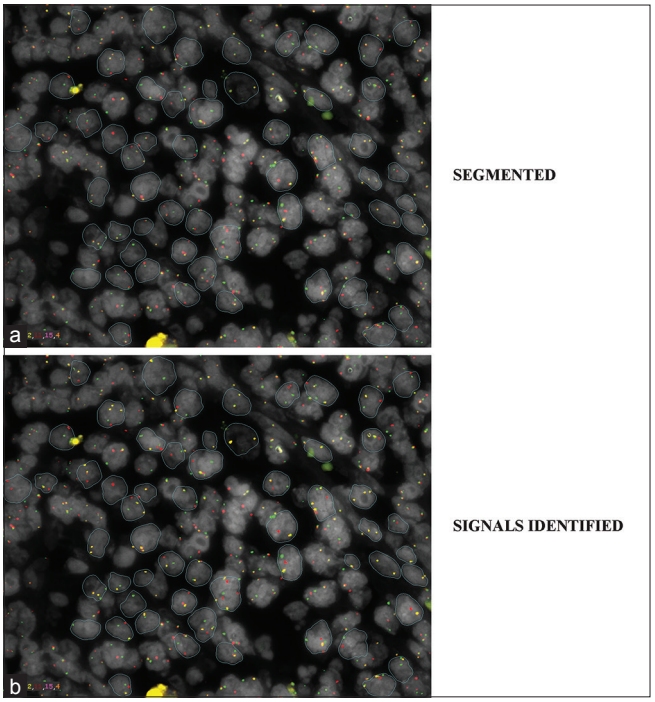

Figure 2:An example of segmented nuclei in a section stained with the LSI-MYC fluorescence *in situ* hybridization probe. (a) Field of view showing segmented nuclei. (b) Same field of view with the signals highlighted by the analysis software

the identification of nuclei, and identified nuclei are circled by the software [Figure 2]. Classification involves the identification of nuclear signal patterns and their tabulation as nonrearranged or rearranged. The software also highlights the signals it identifies. Segmentation and classification are error prone, due to the heterogeneity associated with imaging of tissue sections. The FISH images require manual editing before final analysis, and editing typically involves correcting automated classification errors due to overlapping nuclei or inaccurate nuclear detection. Not all nuclei identified contain signals, and these were also manually excluded from the analysis. Once these nuclei were removed, the remaining nuclei were examined for signal accuracy. The most common error encountered was lack of signal detection. To correct for this error, signals were added or deleted, classifications were changed, and nuclei were manually circled again. Finally, additional nuclei were also manually added to the analysis if there were insufficient nuclei identified by the analysis software. Additional nuclei were chosen if the border could be easily identified (i.e., no overlap).

Data Analysis

Manual fluorescence in situ hybridization

Reference range cutoffs for the manual FISH LSI-MYC and IGH-MYC assays were based on results obtained from normal tissues that were negative for the rearrangements which were a mixture of reactive lymph tissue and normal tonsil/lymph tissue.

Digital LSI-MYC fluorescence in situ hybridization

The analysis software can sort the signal patterns observed into different categories. An example of this is shown in Table 2. Analysis of the LSI-MYC signals was divided into two separate analysis methods. The first looked at the total number of signals that could be used to identify a sample as positive or negative. The second analysis method looked specifically at the percentage of the most common signal pattern (1 fused, 1 green, and 1 orange [1F/1G/1O]) observed in *MYC* 8q24 rearrangements. BETAINV function was used to calculate the normal reference range cutoffs using a 95% confidence level in which nine false-positive cells for the total number of signal patterns and five false-positive cells for the 1F/1G/1O signal pattern were identified among 100 nuclei [Table 3a].

Therefore, samples with ≥23% total rearranged nuclei were considered positive for the *MYC* (8q24) rearrangement. Samples with ≤13% total rearranged nuclei were considered negative for the *MYC* (8q24) rearrangement. When samples had values of total rearranged nuclei between 14% and 23%, the 1F/1G/1O percentage was analyzed. If the 1F1G1O percentage was ≥9%, [Table 3b] the sample was called positive for the *MYC* (8q24) rearrangement. If the 1F/1G/1O percentage was ≤9%, the sample was called borderline for the *MYC* (8q24) rearrangement.[13]

Table 2: Signal configurations used for determining whether a nucleus is rearranged or non-rearranged

Normal	LSI-MYC	IGH-MYC
	2F, 3F, 4F, 5F	2G2O, 2G3O, 3G2O
Rearranged	1F1G1O, 1F1G2O, 1F2G1O, 1F2G2O 2F1G1O, 2F1G2O, 2F2G1O, 2F2G2O, 3F1G1O, 3F1G2O, 3F2G1O 2G2O, 2G3O, 3G2O	1F1G1O, 1F2G2O 1F2G1O, 1F1G2O 2F1G1O, 2F2G1O, 2F1G2O 3F1G1O, 3F2G1O, 3F1G2O 2F 2F1O, 2F1G, 2F2O

F: fused, G: green, O: orange. For the IGH-MYC assay, *IGH* is labeled with green and *MYC* is labeled with orange. At least 1 aqua signal needs to be detected in each nucleus, but is not listed

Table 3a: Results from normal samples used to calculate cutoffs for rearranged LSI-MYC signal counts

Sample	Non-rearranged		Rearranged		Total
	Counts	%	Counts	%	
TS-2	96	96	4	4	100
TS-7	96	96	4	4	100
TS-10	93	93	7	7	100
TS-12	92	92	8	8	100
TS-13	98	98	2	2	100
TS-14	99	99	1	1	100
TS-15	95	95	5	5	100
TS-16	95	95	5	5	100
TS-17	98	98	2	2	100
TS-18	92	92	8	8	100
TS-19	98	98	2	2	100
TS-20	92	92	8	8	100
TS-21	99	99	1	1	100
TS-22	96	96	4	4	100
BL-1 C8	96	96	4	4	100
BL-1 C10	96	96	4	4	100
BL-1 D8	98	98	2	2	100
BL-1 E8	99	99	1	1	100
BL-1 E10	96	96	4	4	100
BL-2 A1	96	96	4	4	100
BL-2 A6	95	95	5	5	100
BL-2 B1	95	95	5	5	100
BL-2 B6	97	97	3	3	100
BETAINV (%)			13		

Digital IGH-MYC fluorescence in situ hybridization

The classic signal pattern expected from tissue with the IGH-MYC rearrangement is 2F/1G/1O 2 aqua (2A). In our laboratory, nuclei containing, at least, 1A signal are counted due to the possibility of truncation due to sectioning. In addition, there is a significant percentage

of single fusion (1F/1G/1O) rearrangements observed in normal cells. Therefore, IGH-MYC signals require looking at the number of both 1F and 2F signals used to identify a sample as positive or negative. 1F signals are defined as having a single fusion and, at least, 1G and 1O signal.

Table 3b: Results from normal samples used to calculate cutoffs for LSI-MYC 1F/1G/1O signal counts, using the BETAINV excel function

Sample	Non-1F/1G/1O		1F/1G/1O		Total
	Counts	%	Counts	%	
TS-2	97	97	3	3	100
TS-7	98	98	2	2	100
TS-10	96	96	4	4	100
TS-12	96	96	4	4	100
TS-13	99	99	1	1	100
TS-14	99	99	1	1	100
TS-15	98	98	2	2	100
TS-16	96	96	4	4	100
TS-17	98	98	2	2	100
TS-18	98	98	2	2	100
TS-19	99	99	1	1	100
TS-20	96	96	4	4	100
TS-21	99	99	1	1	100
TS-22	96	96	4	4	100
BL-1 C8	99	99	1	1	100
BL-1 C10	99	99	1	1	100
BL-1 D8	98	98	2	2	100
BL-1 E8	99	99	1	1	100
BL-1 E10	98	98	2	2	100
BL-2 A1	99	99	1	1	100
BL-2 A6	96	96	4	4	100
BL-2 B1	98	98	2	2	100
BL-2 B6	97	97	3	3	100
BETAINV (%)			9		

2F signals are defined as having, at least, 2F signals and, at least, 1G and 1O signal. Samples with <24% 1F rearranged nuclei and <11% 2F rearranged nuclei were negative for an *MYC* (8q14) rearrangement. Samples with >24% 1F rearranged nuclei or >11% 2F rearranged nuclei were positive for an *MYC* (8q14) rearrangement. BETAINV function was used to calculate the normal reference range cutoffs, using a 95% confidence level in which six false-positive cells for the 2F signal pattern and 22 false-positive cells for the 1F signal pattern were identified among 100 nuclei [Table 4].

RESULTS

The GenASIs capture and analysis system can provide clear images of DAPI stained nuclei and specific hybridized signals [Figure 3]. There are approximately fifty nuclei in each field of view. Such clarity requires diligence in identifying areas with well-defined nuclei exhibiting adequate signal. The overall analysis process is automatic, but there are segmentation and classification parameters which can be manipulated by the user. The required manual editing of the images usually takes about 4 min per frame (field of view image).

Analysis of LSI-MYC by traditional and GenASIs (digital) FISH demonstrated good correlation between the two analysis methods (R^2 = 0.85) [Figure 4]. Each replicate punch in the tissue microarray was analyzed as an individual sample. By traditional FISH analysis, there were twenty nonrearranged, 53 rearranged, and four borderline samples, using a 10% cutoff for negative samples, and a 20% cutoff for positive samples. The BETAINV function was used to calculate normal reference range cutoffs for digital FISH. The GenASIs cutoff was calculated as up to 13% rearranged signals for negative samples and 23% for positive samples. Using the GenASIs

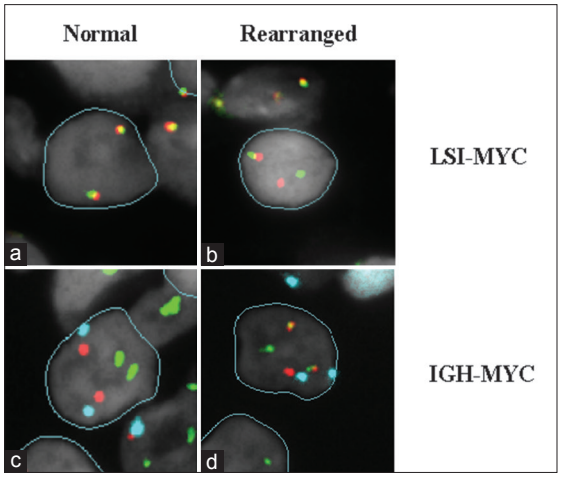

Figure 3: Digital fluorescence *in situ* hybridization images of LSI-MYC and IGH-MYC stained nuclei. (a) Nonrearranged and (b) rearranged nuclei stained with the LSI-MYC fluorescence *in situ* hybridization probe. (c) Nonrearranged and (d) rearranged nuclei stained with the IGH-MYC fluorescence *in situ* hybridization probe

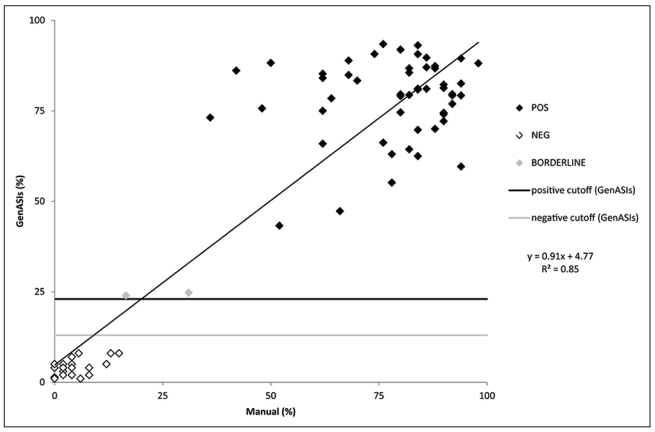

Figure 4: Correlation between the traditional method of analyzing fluorescence *in situ* hybridization and GenASIs capture and analysis system for the LSI-MYC fluorescence *in situ* hybridization probe. Positive (filled), negative (open), and borderline (gray) samples are shown. The positive cutoff for the GenASIs capture and analysis system is shown in black, and the negative cutoff is shown in gray

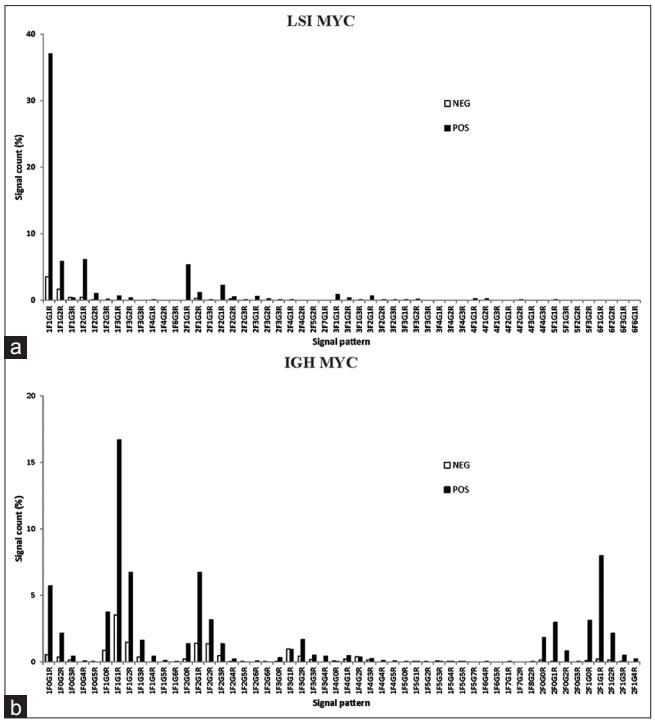

Figure 5: Distribution of rearranged signal patterns observed in positive (filled) and negative (unfilled) samples for the (a) LSI-MYC and (b) IGH-MYC assays

Table 4: Results from normal samples used to calculate cutoffs for IGH-MYC single fusion and dual fusion (1F and 2F) signal counts using the BETAINV excel function

Sample	Non-rearranged		1F		2F		Total
	Counts	%	Counts	%	Counts	%	
TS-1	79	79	2	2	19	19	100
TS-3	78	78	3	3	19	19	100
TS-4	95	95	1	1	4	4	100
TS-5	84	84	1	1	15	15	100
TS-6	92	92	1	1	7	7	100
TS-7	85	85	2	2	13	13	100
TS-9	94	94	1	1	5	5	100
TS-10	79	79	1	1	20	20	100
TS-12	87	87	2	2	11	11	100
TS-14	82	82	0	0	18	18	100
TS-15	79	79	0	0	21	21	100
TS-16	90	90	1	1	9	9	100
TS-17	91	91	0	0	9	9	100
TS-18	89	89	1	1	10	10	100
TS-23	81	81	0	0	19	19	100
TS-24	82	82	2	2	16	16	100
TS-25	85	85	2	2	13	13	100
TS-28	81	81	0	0	19	19	100
TS-32	82	82	1	1	17	17	100
TS-33	77	77	6	6	17	17	100
BETAINV (%)			24		11		

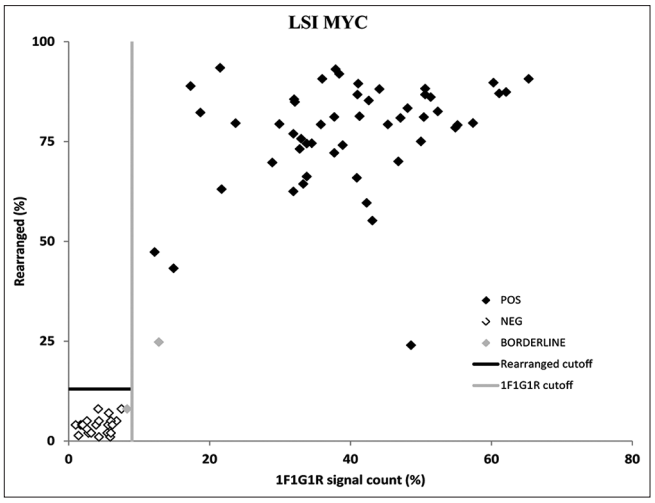

Figure 6: Correlation between the rearranged percentage and specific signal count percentage for the LSI-MYC assay. Positive (filled), negative (open), and borderline (gray) samples are shown. The cutoff for the rearranged percentage is shown in black, and the signal count percentage cutoff is shown in gray

cutoffs, 100% (53/53) positive samples, 85% (17/20) negative samples, and 50% (2/4) borderline samples were accurately classified for a 94% rate of correlation between GenASIs and traditional FISH analysis methods.

The most common signal pattern observed for LSI-MYC was 1F/1G/1O [Figure 5]. The BETAINV function from the twenty negative samples was used to calculate the 1F/1G/1O cutoff, which was found to be 9%. Plotting the GenASIs results against the 1F/1G/1O results demonstrated good separation between positive and negative samples [Figure 6]. Using 10% as the negative cutoff for the 1F/1G/1O signal count, each borderline sample in the validation was reclassified as negative. Combining the analysis, the cutoffs were as follows: Samples with ≥23% total rearranged nuclei were considered positive for the *MYC* (8q24) rearrangements, samples with <13% total rearranged nuclei were considered negative for the *MYC* (8q24) rearrangements, and samples with 13–22% total rearranged nuclei were considered borderline for the *MYC* (8q24) rearrangement if the 1F/1G/1O rearranged nuclei represented <9% of the nuclei. Cases where 1F/1G/1O rearranged nuclei represented ≥9% of the total counted could be diagnosed as positive at the discretion of the reviewing staff pathologist.

With regard to the IGH-MYC results, there was a good correlation between the two different analysis methods ($R^2 = 0.95$) [Figure 7]. By traditional FISH, 20% cutoff was used for 1F or 2F rearranged cells between positive and negative samples. The BETAINV function was used to calculate cutoffs for digital FISH. The GenASIs cutoff was calculated as samples with <24% 1F rearranged nuclei and <11% 2F rearranged nuclei were

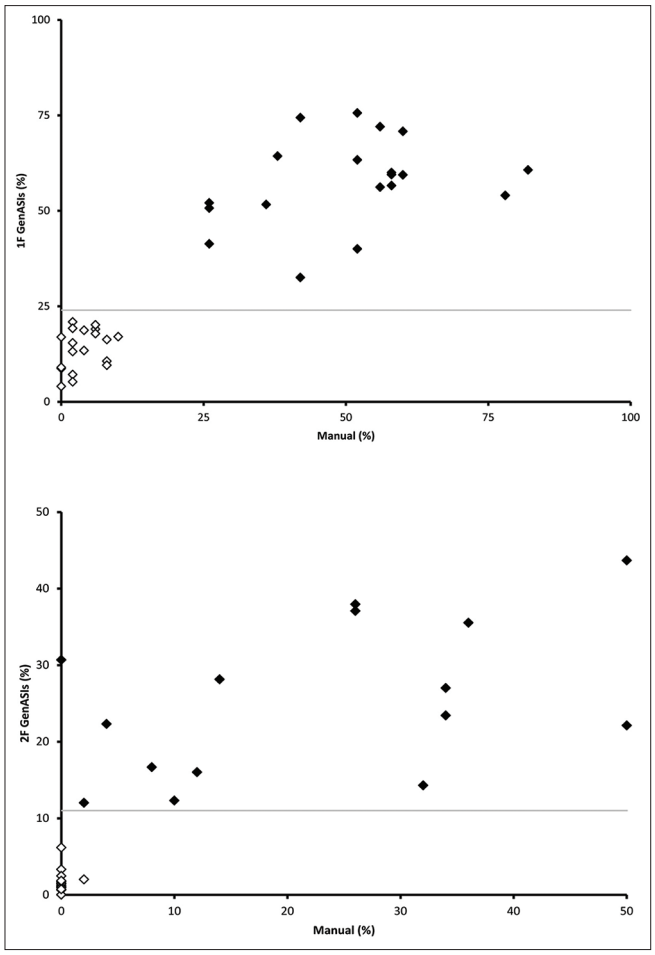

Figure 7: Correlation between the traditional method of analyzing fluorescence *in situ* hybridization and GenASIs capture and analysis system for the IGH-MYC fluorescence *in situ* hybridization probe. Positive (filled) and negative (open) samples are shown. The 1 fused and 2 fused rearranged cutoff for the GenASIs capture and analysis system are shown in gray

negative for an *MYC* (8q14) rearrangement. Samples with >24% 1F rearranged nuclei or >11% 2F rearranged nuclei were positive for *MYC* (8q14) rearrangement. Using the GenASIs cutoffs, 100% (20/20) positive samples and 100% (20/20) negative samples were accurately classified for a 100% rate of correlation between GenASIs and traditional FISH.

For the IGH-MYC assay, the rearranged signal patterns were more widely distributed [Figure 5]. The most abundant signal pattern was 1F/1G/1O, with 1F/1G/2O, 1F/2G/1O and 2F/1G/1O having lower but significant levels. Theoretically, the 2F signal patterns should be associated with rearrangements but, in our cases, these signal patterns were not as predominant as the 1F signal patterns. The BETAINV function was used to calculate a cutoff for the 1F and 2F signal patterns. Comparing the GenASIs results to the manual results, there was a good correlation between positive and negative samples when looking at either signal patterns [Figure 7]. One-hundred percent (19/19) of samples that were positive by the manual method were positive using the GenASIs cutoff for the single fusion and dual fusion signal patterns. One-hundred percent (20/20) of samples that were negative by the manual method were negative using the GenASIs cutoff for the single fusion and dual fusion patterns.

The validation identified two cases (one LSI-MYC and one IGH-MYC) which were initially diagnosed as negative by gold-standard traditional FISH analysis and subsequently found to be positive by digital FISH analysis. Upon review, areas of positivity and negativity were present within these LSI-MYC and IGH-MYC cases, indicating the importance of adequate tissue matching before segmentation and classification. These cases were not included in calculation of the cutoffs.

DISCUSSION

FISH is a well-established method in pathology laboratories,[14,15] and it is a relatively robust technique, with an added advantage of use on archived FFPE tissue specimens when fresh tissue is not available.[8] Both break-apart and dual fusion FISH probes have their own unique advantages and disadvantages for use in diagnostic assays.[7] One study evaluated the differences between break-apart and dual fusion probes and concluded that dual fusion probes have a lower false positivity rate.[16] If only a break-apart probe is available for a particular gene, the distance between signals with relation to the signal diameter needs to be well characterized for nonrearranged samples to make the assay as accurate as possible.

We demonstrated good correlation between traditional and digital FISH analysis for *MYC* rearrangements using both LSI break-apart and IGH-MYC fusion probes. Our findings document improved diagnostic accuracy with the implementation of digital FISH analysis, highlighted by the samples that were re-classified as positive by digital FISH analysis. Segmented and classified digital images allow for permanent storage of analyzed specimens and easy accessibility for further review and/or educational purposes. The digital platform is also conducive to laboratory workflow as it allows for timely segmentation and classification of nuclei, remote access for review of cases, elimination of manual slide transportation, and accurate identification/assessment of tumor from digital tissue matching.

Our results are in good agreement with previous studies that have also looked at automated analysis of FISH results from FFPE BCL tissue.[12,16] The automated analysis yielded 100% agreement with conventional FISH in both studies. In contrast, the amount of time it takes to analyze a sample is significantly different. Our average analysis time is approximately 19 min while it was reported that the average analysis time was 9 min using

a Metafer 4 scanning system (MetaSystems, Altlussheim, Germany).[16] The difference is due to the manual editing required when using the GenASIs system, which was not required when using the Metafer 4 scanning system.

The rearranged signal patterns recorded for the LSI-MYC assay were consistent with what is expected (predominantly 1F/1G/1O). However, the dominant rearranged signal pattern identified with IGH-MYC assay was 1F/1G/1O, and often, but less frequently, the 2F/1G/1O signal was present alongside 1F/2G/1O and 1F/1G/2O. At this point, it is assumed that the abundance of 1F/1G/1O is due to loss of one of the fusions during sectioning. The sample with a positive rearrangement percentage but a negative 2F/1F/1O percentage also failed to have an abundance of 1F/1G/1O signals. This case exhibited an even distribution among other rearranged signal patterns. Unlike LSI-MYC, a single signal pattern cannot be used as a discriminator in IGH-MYC cases. The different signal patterns could indicate genetic differences between tumors that have 1F/1G/1O as the most abundant signal. A more extensive study involving more clinical data and samples is required to evaluate clinical significance.

Aside from Burkitt lymphoma, *MYC* rearrangements detection will continue to be of diagnostic and clinical significance in aggressive large BCLs which harbor *MYC* rearrangements alongside rearrangements in the anti-apoptotic gene *BCL2* or transcriptional repressor *BCL6*. Lymphomas which harbor an *MYC* rearrangement plus a BCL2 or BCL6 rearrangement are termed double hit large BCLs (double-hit lymphoma) and those with rearrangements in all three genes are termed triple hit large BCLs triple-hit lymphoma (THL). Each of these is associated with a very poor clinical prognosis in comparison to large BCLs without identifiable translocations involving *MYC* with or without *BCL2* and *BCL6*.[17,18] For these reasons, sensitive, specific, and accurate detection of all three gene rearrangements is essential for diagnosis, appropriate clinical therapy, and overall patient care.

No single FISH probe can cover all of the possible *MYC* rearrangements, and more complex rearrangements can be missed.[19-21] The detection rate of *MYC* rearrangements has been reported to be approximately 10% in DLBCL.[18,22-24] It has also been reported that the incidence of detection increases to 30% when using immunohistochemistry[17] indicating that detection of protein overexpression needs to be a part of a panel of testing to make the detection of DHL and THL optimal. There is no current standardized best practice for FISH testing in lymphomas. A recommendation on how to standardize FISH testing in multiple myeloma has been published[25] and would provide a good framework for lymphoma testing.

Based on the literature, eighty percent of the translocations observed in Burkitt lymphoma is between *MYC* and *IGH*, but other translocation partners have been reported as well.[26] Other partners of *MYC* include other IG chain loci such as kappa light chain (IGK) and the lambda light chain (IGL). It has been reported that approximately 5–14% of DLBCL have *MYC* rearrangements.[27,28] The translocation partner of *MYC* appears to be dependent on the type of lymphoma. Therefore, similarly to what is observed in Burkitt lymphoma, *MYC* and IGH can also be rearranged in DLBCL.[5,6,26] However, in T-acute lymphoblastic leukemia/lymphoma, there is *MYC* involvement with T-cell receptor alpha/delta and, in plasma cell myeloma, the translocation partner is IGK and IGL.[23,29] There are also differences in the frequency of expression between lymphoma types. For example, the immunoblastic variant of DLBCL has been reported to have an *MYC* rearrangement in 33% of cases versus 7% in nonimmunoblastic DLBCL variants.[30]

The primary cost of switching over to a digital FISH system from a manual system is the new hardware including computer, scanning system, and slide loaders. The digital FISH system increases the cost of a stand-alone epifluorescence microscope, by about 10-fold. Depending on whether whole slide images are captured, or just a few fields of view, additional computer servers may be needed for data storage. One may expect that if the digital FISH analysis is completely automated and the results are 100% accurate, it is faster than manual FISH analysis. From our experience, the results are not 100% accurate and a large amount of time needs to be spent manually editing the results. On average, with the current system, it can take approximately 19 min to analyze a sample using the digital FISH analysis compared to 5 min for manual FISH analysis.

There are several future considerations that arise from developing digital FISH imaging. Whole slide imaging of H and E slides is a powerful technique and is a possible application in digital FISH imaging. Similar to imaging an entire H and E slide, it would mean that the entire section could be analyzed, minimizing the possibility that a small area of tumor may be missed. However, FISH slides need to be analyzed under higher magnification (at least ×60) to maintain the resolution between signals, which makes the scanning time longer, and the image files extremely large, making data storage an issue. The Food and Drug Administration concerns over digital pathology will affect future regulation of digital FISH analysis. Validated assays need to be developed to demonstrate that there is no loss of accuracy using a computer versus an epifluorescence microscope, because there are serious consequences for misdiagnosis if the images are not used properly. Image formats, resolution, and compression are important factors in accurate interpretation of digital FISH images. For the most accurate digital FISH data, images that do not lose data during compression (i.e., TIF LZW or PNG) should be used. The drawback is that data storage

becomes an issue, since files stay large but is important to maintain image quality and accuracy.

Digital capture and analysis of FISH assays are a positive development for this important laboratory testing modality. The *MYC* FISH assays which we have converted to our GenASIs digital imaging platform have provided numerous logistical and diagnostic advantages as indicated previously. In addition, individual signal patterns can be recorded and stored. These data alongside advances in computational power can potentially lead to correlation between signal pattern and unique tumor phenotypes or overall tumor prognosis. There are still limitations to digital FISH analysis, in particular being able to reliably identify nuclei and hybridized signal. However, since the resolution of digital FISH images will only increase, and the algorithms used for detection of nuclei and signals will continually be refined, digital FISH analysis can only improve. As indicated, we feel that digital FISH analysis provides more efficient and accurate results and better patient care in comparison to traditional FISH methods. Efforts to convert other FFPE-based FISH assays to this digital platform are underway in our laboratory.

Financial Support and Sponsorship
Nil.

Conflicts of Interest
There are no conflicts of interest.

REFERENCES

1. Braziel RM, Arber DA, Slovak ML, Gulley ML, Spier C, Kjeldsberg C, *et al.* The Burkitt-like lymphomas: A Southwest Oncology Group study delineating phenotypic, genotypic, and clinical features. Blood 2001;97:3713-20.
2. Kanungo A, Medeiros LJ, Abruzzo LV, Lin P. Lymphoid neoplasms associated with concurrent t(14;18) and 8q24/c-MYC translocation generally have a poor prognosis. Mod Pathol 2006;19:25-33.
3. Rodig SJ, Vergilio JA, Shahsafaei A, Dorfman DM. Characteristic expression patterns of TCL1, CD38, and CD44 identify aggressive lymphomas harboring a MYC translocation. Am J Surg Pathol 2008;32:113-22.
4. Seegmiller AC, Garcia R, Huang R, Maleki A, Karandikar NJ, Chen W. Simple karyotype and bcl-6 expression predict a diagnosis of Burkitt lymphoma and better survival in IG-MYC rearranged high-grade B-cell lymphomas. Mod Pathol 2010;23:909-20.
5. Copie-Bergman C, Cuillière-Dartigues P, Baia M, Briere J, Delarue R, Canioni D, *et al.* MYC-IG rearrangements are negative predictors of survival in DLBCL patients treated with immunochemotherapy: A GELA/LYSA study. Blood 2015;126:2466-74.
6. Pedersen MØ, Gang AO, Poulsen TS, Knudsen H, Lauritzen AF, Nielsen SL, *et al.* MYC translocation partner gene determines survival of patients with large B-cell lymphoma with MYC- or double-hit MYC/BCL2 translocations. Eur J Haematol 2014;92:42-8.
7. Ventura RA, Martin-Subero JI, Jones M, McParland J, Gesk S, Mason DY, *et al.* FISH analysis for the detection of lymphoma-associated chromosomal abnormalities in routine paraffin-embedded tissue. J Mol Diagn 2006;8:141-51.
8. Muñoz-Mármol AM, Sanz C, Tapia G, Marginet R, Ariza A, Mate JL. MYC status determination in aggressive B-cell lymphoma: The impact of FISH probe selection. Histopathology 2013;63:418-24.
9. Martín-Subero JI, Gesk S, Harder L, Grote W, Siebert R. Interphase cytogenetics of hematological neoplasms under the perspective of the novel WHO classification. Anticancer Res 2003;23:1139-48.
10. Yoon N, Do IG, Cho EY. Analysis of HER2 status in breast carcinoma by fully automated HER2 fluorescence *in situ* hybridization (FISH): Comparison of two immunohistochemical tests and manual FISH. APMIS 2014;122:755-60.
11. van der Logt EM, Kuperus DA, van Setten JW, van den Heuvel MC, Boers JE, Schuuring E, *et al.* Fully automated fluorescent *in situ* hybridization (FISH) staining and digital analysis of HER2 in breast cancer: A validation study. PLoS One 2015;10:e0123201.
12. Reichard KK, Hall BK, Corn A, Foucar MK, Hozier J. Automated analysis of fluorescence *in situ* hybridization on fixed, paraffin-embedded whole tissue sections in B-cell lymphoma. Mod Pathol 2006;19:1027-33.
13. Wiktor AE, Van Dyke DL, Stupca PJ, Ketterling RP, Thorland EC, Shearer BM, *et al.* Preclinical validation of fluorescence *in situ* hybridization assays for clinical practice. Genet Med 2006;8:16-23.
14. Haralambieva E, Schuuring E, Rosati S, van Noesel C, Jansen P, Appel I, *et al.* Interphase fluorescence *in situ* hybridization for detection of 8q24/MYC breakpoints on routine histologic sections: Validation in Burkitt lymphomas from three geographic regions. Genes Chromosomes Cancer 2004;40:10-8.
15. van Rijk A, Mason D, Jones M, Cabeçadas J, Crespo M, Cigudosa JC, *et al.* Translocation detection in lymphoma diagnosis by split-signal FISH: A standardised approach. J Hematop 2008;1:119-26.
16. Alpár D, Hermesz J, Pótó L, László R, Kereskai L, Jáksó P, *et al.* Automated FISH analysis using dual-fusion and break-apart probes on paraffin-embedded tissue sections. Cytometry A 2008;73:651-7.
17. Petrich AM, Nabhan C, Smith SM. MYC-associated and double-hit lymphomas: A review of pathobiology, prognosis, and therapeutic approaches. Cancer 2014;120:3884-95.
18. Horn H, Ziepert M, Becher C, Barth TF, Bernd HW, Feller AC, *et al.* MYC status in concert with BCL2 and BCL6 expression predicts outcome in diffuse large B-cell lymphoma. Blood 2013;121:2253-63.
19. Einerson RR, Law ME, Blair HE, Kurtin PJ, McClure RF, Ketterling RP, *et al.* Novel FISH probes designed to detect IGK-MYC and IGL-MYC rearrangements in B-cell lineage malignancy identify a new breakpoint cluster region designated BVR2. Leukemia 2006;20:1790-9.
20. Joos S, Haluska FG, Falk MH, Henglein B, Hameister H, Croce CM, *et al.* Mapping chromosomal breakpoints of Burkitt's t(8;14) translocations far upstream of c-myc. Cancer Res 1992;52:6547-52.
21. Nagel I, Akasaka T, Klapper W, Gesk S, Böttcher S, Ritgen M, *et al.* Identification of the gene encoding cyclin E1 (CCNE1) as a novel IGH translocation partner in t(14;19)(q32;q12) in diffuse large B-cell lymphoma. Haematologica 2009;94:1020-3.
22. Akyurek N, Uner A, Benekli M, Barista I. Prognostic significance of MYC, BCL2, and BCL6 rearrangements in patients with diffuse large B-cell lymphoma treated with cyclophosphamide, doxorubicin, vincristine, and prednisone plus rituximab. Cancer 2012;118:4173-83.
23. Barrans S, Crouch S, Smith A, Turner K, Owen R, Patmore R, *et al.* Rearrangement of MYC is associated with poor prognosis in patients with diffuse large B-cell lymphoma treated in the era of rituximab. J Clin Oncol 2010;28:3360-5.
24. Savage KJ, Johnson NA, Ben-Neriah S, Connors JM, Sehn LH, Farinha P, *et al.* MYC gene rearrangements are associated with a poor prognosis in diffuse large B-cell lymphoma patients treated with R-CHOP chemotherapy. Blood 2009;114:3533-7.
25. Ross FM, Avet-Loiseau H, Ameye G, Gutiérrez NC, Liebisch P, O'Connor S, *et al.* Report from the European Myeloma Network on interphase FISH in multiple myeloma and related disorders. Haematologica 2012;97:1272-7.
26. Boxer LM, Dang CV. Translocations involving c-myc and c-myc function. Oncogene 2001;20:5595-610.
27. Karube K, Campo E. MYC alterations in diffuse large B-cell lymphomas. Semin Hematol 2015;52:97-106.
28. Ott G, Rosenwald A, Campo E. Understanding MYC-driven aggressive B-cell lymphomas: Pathogenesis and classification. Hematology Am Soc Hematol Educ Program 2013;2013:575-83.
29. Bernard O, Larsen CJ, Hampe A, Mauchauffé M, Berger R, Mathieu-Mahul D. Molecular mechanisms of a t(8;14)(q24;q11) translocation juxtaposing c-myc and TcR-alpha genes in a T-cell leukaemia: Involvement of a V alpha internal heptamer. Oncogene 1988;2:195-200.
30. Horn H, Staiger AM, Vöhringer M, Hay U, Campo E, Rosenwald A, *et al.* Diffuse large B-cell lymphomas of immunoblastic type are a major reservoir for MYC-IGH translocations. Am J Surg Pathol 2015;39:61-6.